HOME | ABOUT ⌄ | CONTRIBUTE ⌄ | BROWSE ⌄

About Microwave and Optical Technology Letters

Microwave and Optical Technology Letters provides quick publication (3 to 6 month turnaround) of the most recent findings and achievements in high frequency technology, from RF to optical spectrum. The journal publishes original short papers and letters on theoretical, applied, and system results in RF, Microwave, and Millimeter Waves, Antennas and Propagation, Submillimeter-Wave and Infrared Technology, and Optical Engineering.

Read the journal's full aims and scope.

Submit an Article

Browse free sample issue

Get content alerts

Recommend to a librarian

Subscribe to this journal

Editorial Board

EDITOR

Kai Chang (Texas A&M University, College Station, USA)

EDITORIAL BOARD

F. Gardiol (Ecole Polytechnique Federale, Switzerland)
H. Ghafouri-Shiraz (University of Birmingham, England)
J. Goel (Raytheon SAS, USA)
P. F. Goldsmith (Cornell University, USA)

K. Peterman (Technical University, Berlin, Germany)
J. Ra (KAIST, Korea)
I. Robertson (University of Surrey, UK)
A. Rosen (Drexel University, USA)
G. Salmer (Universitéé des Sciences et

R. C. Hansen (Consultant, USA)
A. Hardy (Tel Aviv University, Israel)
J. F. Harvey (Army Research Office, USA)
P. R. Herczfeld (Drexel University, USA)
W. J. R. Hoefer (University of Victoria, Canada)
H. C. Huang (Shanghai Science Technology University, China)
C. Jackson (Raytheon SAS, USA)
D. Jager (Gerhard-Mercator Universitat, Germany)
R. Jansen (Industrial Microwave and RF Techniques Inc., Germany)
J.M. Jin (University of Ilinois, USA)
M.A. Karim (The City University of New York, USA)
L. P. B. Katehi (University of Michigan, USA)
E. L. Kollberg (Chalmers University of Technology, Sweden)
J. A. Kong (MIT, USA)
Y. Konishi (K. Laboratory Co., Ltd., Japan)
S. K. Koul (Indian Institute of Technology, India)
H. J. Kuno (Quin Star Technology, USA)
A. Lakhtakia (Pennsylvania State University, USA)
C. H. Lee (University of Maryland, USA)
J. N. Lee (Naval Research Labs, USA)

T.K. Sarkar (Syracuse University, USA)
F. K. Schwering (US Army CECOM, USA)
A. Seeds (University College London, UK)
A. K. Sharma (TRW, USA)
L. C. Shen (University of Houston, USA)
D. W. Smith (Corning Research Centre, England)
B. E. Spielman (Washington University in St. Louis, USA)
C. Sun (California Polytechnic State University, USA)
C. S. Tsai (University of California at Irvine, USA)
L. Tsang (University of Washington, USA)
H. Q. Tserng (Texas Instruments, USA)
J. B. Y. Tsui (Wright-Patterson AFB, USA)
A. V. Vorst (Catholic University, Belgium)
O. Wada (Kobe University)
R. W. Wang (Academia Sinica, China)
B. Wilhelmi (Jenoptik AG, Germany)
A. G. Williamson (University of Auckland, New Zealand)
J. C. Wiltse (Georgia Technology Research Institute, USA)
K.L. Wong (National Sun Yat-Sen University, Taiwan)
J. Wu (National Taiwan University, Taiwan)
K. Wu (Ecole Polytechnique de Montreal, Canada)
E. Yamashita (University of Electro-Communications, Japan)
S. K. Yao (Optech, USA)
H. W. Yen (Hughes Research Labs, USA)
F. T. S. Yu (Pennsylvania State University, USA)
E. Yung (City University of Hong Kong, Hong Kong)
W.X. Zhang (Nanjing, China)

HOME ABOUT ∨ CONTRIBUTE ∨ BROWSE ∨

Volume 61, Issue 1

Pages: 1-285
January 2019

Submit an Article

Browse free sample issue

Get content alerts

Recommend to a librarian

Subscribe to this journal

More from this journal

- Resources for Authors
- Wiley Job Network

≔ GO TO SECTION

ISSUE INFORMATION

🔓 Free Access

Issue Information

Pages: 1-4 | First Published: 13 December 2018

First Page | PDF | Request permissions

RESEARCH ARTICLES

Robust real-time inversion of electrical impedance tomography data for human lung ventilation monitoring

Marco Salucci, Giacomo Oliveri

Pages: 5-8 | First Published: 14 November 2018

Abstract | Full text | PDF | References | Request permissions

A compact low-phase noise oscillator using π-network and complimentary μ-near zero metamaterial resonator

Ki-Cheol Yoon, Seungyoung Ahn, Jong-Chul Lee

Pages: 9-14 | First Published: 01 November 2018

Abstract | Full text | PDF | References | Request permissions

Measurement of the electromagnetic properties of thin-films using a microwave resonant cavity

Radwan Dib, Didier Vincent, Ahmad Elrafhi

Pages: 15-19 | First Published: 11 November 2018

Abstract | Full text | PDF | References | Request permissions

Multiple-input and multiple-output antenna system with self-isolated antenna element for fifth-generation mobile terminals

Anping Zhao, Zhouyou Ren

Pages: 20-27 | First Published: 11 November 2018

Abstract | Full text | PDF | References | Request permissions

Non-touch detection of rhodamine B concentration in distilled water using fiber coupler based on displacement sensor

Samian, A. H. Zaidan, M. P. Anggraeni, M. Yasin, Supadi

Pages: 223-228 | First Published: 01 November 2018

Abstract | Full text | PDF | References | Request permissions

---

A coupled-fed dual-band impedance matching network for small long-term evolution smartphone antennas

Duo-Long Wu, Jian-Feng Li, Yan Jie Wu

Pages: 229-234 | First Published: 22 November 2018

Abstract | Full text | PDF | References | Request permissions

---

An 80-100 GHz VCO using auxiliary cross-coupled pair and push-push topology in 0.18-μm CMOS

Jui-Chi Huang, Sen Wang, Ting-Yi Tsai

Pages: 235-238 | First Published: 23 November 2018

Abstract | Full text | PDF | References | Request permissions

---

A self-diplexing MIMO antenna for WLAN applications

Sourav Nandi, Akhilesh Mohan

Pages: 239-244 | First Published: 23 November 2018

Abstract | Full text | PDF | References | Request permissions

---

A compact reconfigurable ultra-wideband G-shaped printed antenna with band-notched characteristic

Abdurrahim Toktas, Mehmet Yerlikaya

Pages: 245-250 | First Published: 01 November 2018

Abstract | Full text | PDF | References | Request permissions

---

Quasi blind carrier phase estimation scheme for special-shaped circular (7,1) modulation in high-speed visible light communication

Shangyu Liang, Jiaqi Zhao, Yingjun Zhou, Mengjie Zhang, Nan Chi

Pages: 251-255 | First Published: 14 November 2018

Abstract | Full text | PDF | References | Request permissions

Microwave and Optical Technology Letters

Country	United States

Subject Area and Category	Engineering
	    Electrical and Electronic Engineering
	
	Materials Science
	    Electronic, Optical and Magnetic Materials
	
	Physics and Astronomy
	    Atomic and Molecular Physics, and Optics
	    Condensed Matter Physics

Publisher	John Wiley & Sons Inc.
Publication type	Journals
ISSN	10982760, 08952477
Coverage	1988-ongoing
Scope	Microwave and Optical Technology Letters provides quick publication (3 to 6 month turnaround) of the most recent findings and achievements in high frequency technology, from RF to optical spectrum. The journal publishes original short papers and letters on theoretical, applied, and system results in the following areas. - RF, Microwave, and Millimeter Waves - Antennas and Propagation - Submillimeter-Wave and Infrared Technology - Optical Engineering All papers are subject to peer review before publication

67

H Index

⑦ How to publish in this journal

💬 Join the conversation about this journal

Quartiles +

SJR +	Citations per document +

Total Cites   Self-Cites

External Cites per Doc   Cites per Doc

% International Collaboration

Cites / Doc. (4 years)
Cites / Doc. (3 years)
Cites / Doc. (2 years)

Citable documents   Non-citable documents

Cited documents   Uncited documents

Microwave and Optical Technology Letters

Q3 Atomic and Molecular Physics, and Optics
best quartile
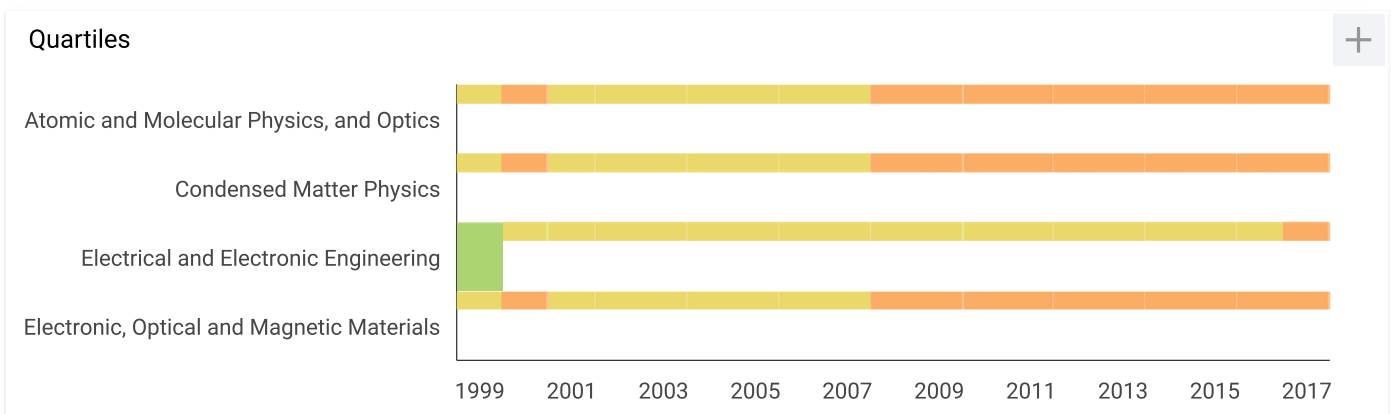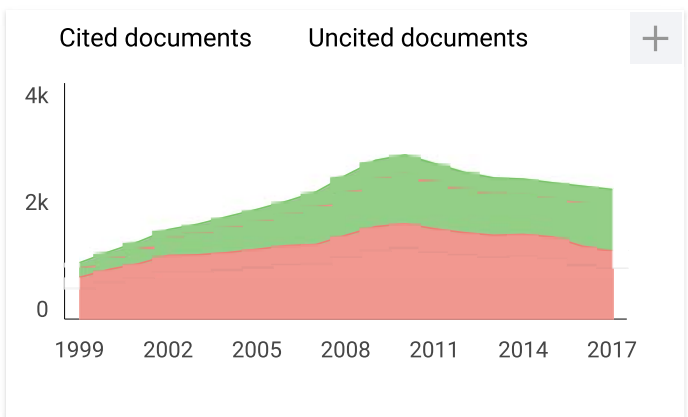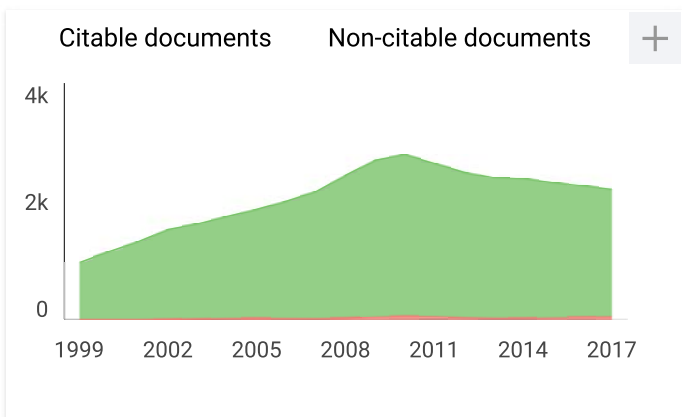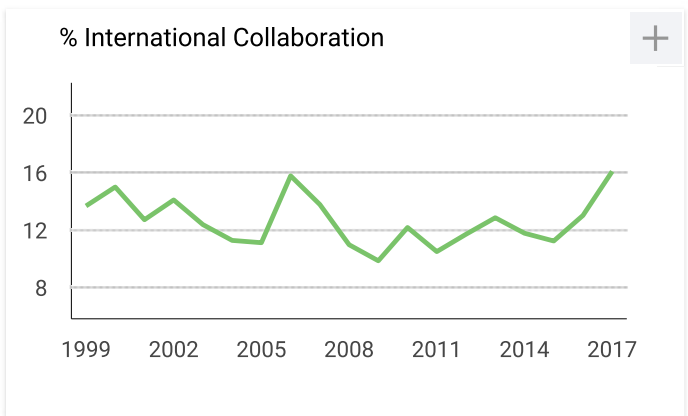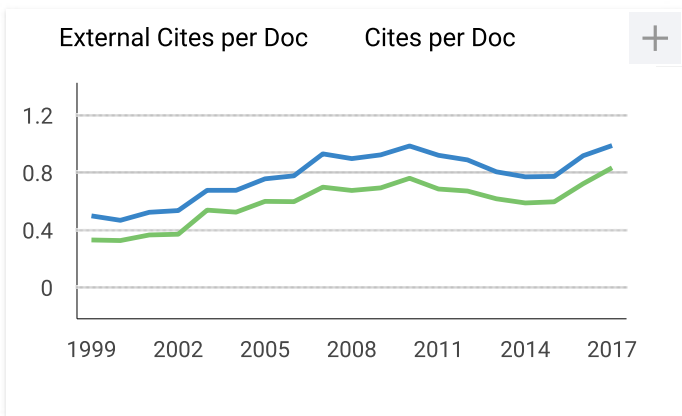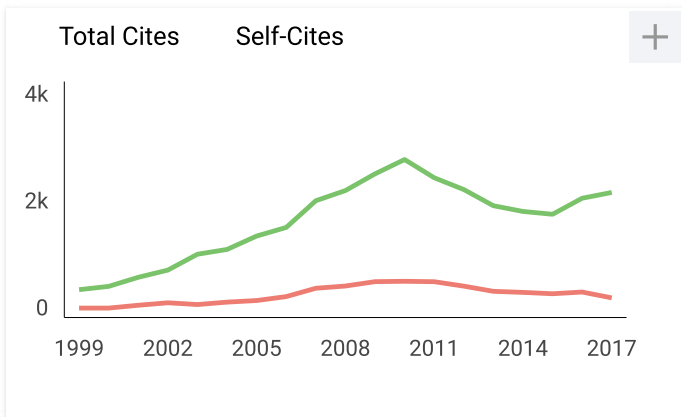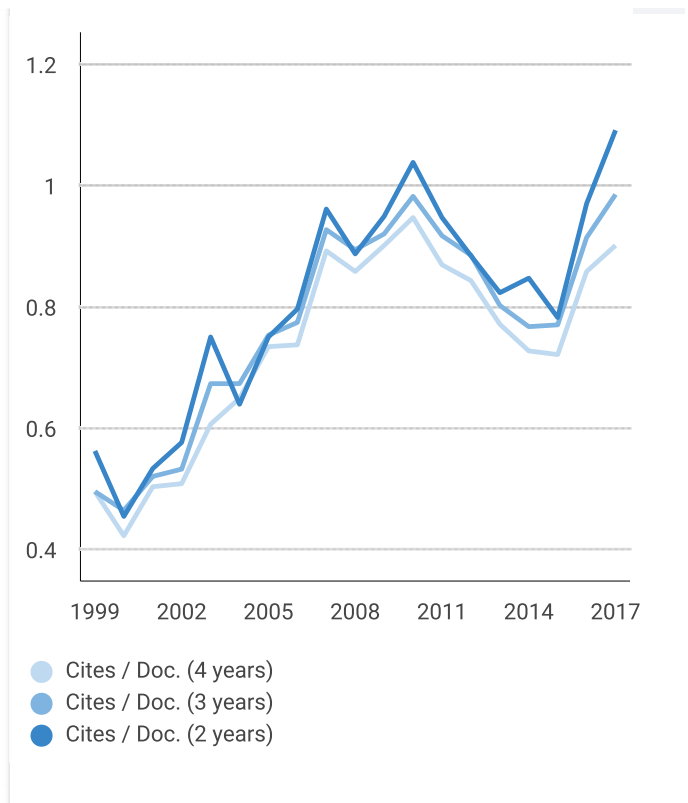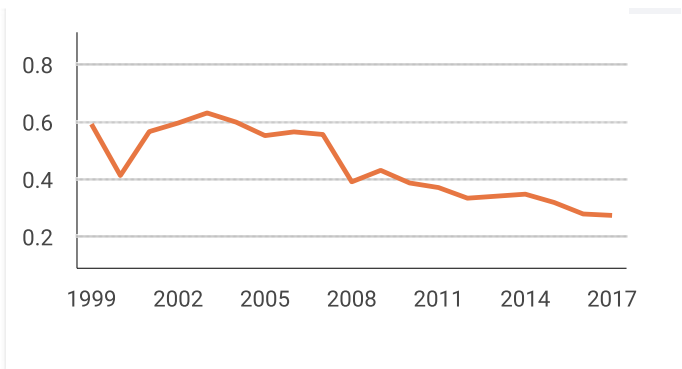
SJR 2017
0.27

powered by scimagojr.com

← Show this widget in your own website

Just copy the code below and paste within your html code:

`<a href="https://www.scimag`

Leave a comment

Name

Email

(will not be published)

Submit

The users of Scimago Journal & Country Rank have the possibility to dialogue through comments linked to a specific journal. The purpose is to have a forum in which general doubts about the processes of publication in the journal, experiences and other issues derived from the publication of papers are resolved. For topics on particular articles, maintain the dialogue through the usual channels with your editor.

WILEY

Non-touch detection of rhodamine B concentration in distilled water using fiber coupler based on displacement sensor

Samian [ID] | A. H. Zaidan |

M. P. Anggraeni | M. Yasin | Supadi

Physics Department, Faculty of Science and Technology, Universitas Airlangga, Surabaya, Indonesia

Correspondence
Samian, Physics Department, Faculty of Science and Technology, Universitas Airlangga, 60115 Surabaya, Indonesia.
Email: samian@fst.unair.ac.id

Abstract

Non-touch detection of rhodamine B concentration in distilled water using fiber coupler and concave mirror (CM) successfully demonstrated. Based on displacement sensor, the concentration of rhodamine B is detected through the peak voltage value which is resulted from the displacement profile. Using the He-Ne (543 nm) laser as the source, the fiber coupler as the sensor probe and CM with the curvature radius of 12 mm as the reflector as well as the sample container, the rhodamine B concentration can be detected in the range 0-20 ppm and the resolution of 0.26 ppm.

KEYWORDS

concave mirror, displacement sensor, fiber coupler, non-touch detection

1 | INTRODUCTION

The development of refractive index and substance concentration sensor has been done with various methods and configurations. Reflection method using mirror (flat or concave) has been used to detect the refractive index of the liquid,[1] calcium concentration,[2] sodium chloride,[3]

glucose,[4,5] rhodamine B,[6] and magnesium[7] using fiber bundle[1–4] or fiber coupler[5–7] as the sensor probe. The working mechanism of the refractive index and substance concentration sensor is based on displacement sensor, that is, by shifting the sensor probe against the mirror with the solution being made as a medium between sensor probe and mirror. The detection of the refractive index and substance concentration is conducted through the peak voltage value[1–4,6,7] or maximum voltage[5] of optical detector resulted from the shift of the sensor probe to the mirror. Side-emitting technique is successfully applied to detect the refractive index of chlorinated water[8] and the concentration of uric acid[9] using microbend and tapered fiber optic as sensor probe, respectively. The detection mechanism is carried out through changes in light intensity guided in microbend or tapered fiber optic due to changes in the refractive index or the content of the solution on the side of microbend or tapered fiber optic. For the detection method of the sensor using reflection technique and side-emitting, the working principle utilizes refraction,[1–5,8,9] absorption,[6] or refraction as well as absorption[7] of light due to interaction with the solution. Another method has been developed based on surface plasmon resonance (SPR) using silver-coated fiber optic[10] and Nano composite of ZnO-polypyrrol[11] as a sensor probe, each capable of detecting the concentration of uric acid and manganese ions. The detection mechanism of the substance concentration is carried out through the wavelength spectrum of the sensor probe interaction results with the sample.

The working mechanism of the refractive index and substance concentration sensor requires that the sensor probe to be immersed to the sample solution. Direct contact between the sensor probe and the solution required cleaning up procedure due to remnants of the adhesive solution on the sensor probe which will disturb sensor performance when it will be used again. It becomes problematic if the detected solution is difficult to clean from the sensor probe and thus requires a new probe. In this paper, we propose the rhodamine B concentration sensor in distilled water using a fiber coupler as a probe sensor with concave mirror (CM) as a reflector as well as a sample container. Based on displacement sensor, the detection mechanism does not need direct contact (non-touch) between sensor probes and samples. With non-touch mechanism, the proposed sensor is suitable for rhodamine B solutions or other solutions that are difficult to clean from the sensor probe.
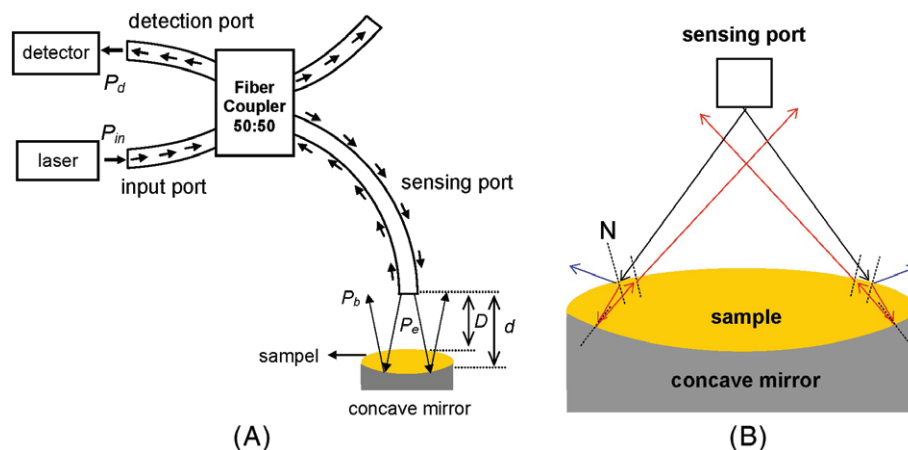
FIGURE 1 (A) The design of the rhodamine B concentration sensor using a fiber coupler with CM as the reflector as well as the sample container and (B) an alternate light propagation illustration between the CM sample-port sensing [Color figure can be viewed at wileyonlinelibrary.com]

2 | SENSOR WORK MECHANISM

Figure 1A shows the design of rhodamine B concentration sensor in distilled water using fiber coupler as sensor probe and CM as reflector as well as sample container. Volume of sample (rhodamine B solution) used is small, which is almost twice the volume of CM and structure resembles a convex lens. Therefore, the detected solution must be meniscus (the cohesion force is greater than the adhesion force) in order not to spill from the sample container.

The laser light trajectory in our set-up is as follows, after laser light enters the input port of the fiber coupler (P_{in}) in Figure 1A, half of it is passed by the sensing port (P_e) through the sample to the CM. In this case, the sensing port of the fiber coupler serves as the sensor probe. The reflected light from CM once again penetrates the solution and some will return to the sensing port (P_b). Half of the light intensity that enters back to the sensing port will be forwarded to the optical detector through the detection port (P_d). The intensity of light entering the optical detector is read in the form of the output voltage of the detector. If there is no sample, the sensor probe shift against CM (d) will result in a peak voltage when the probe position of the sensor is around the curvature radius of CM.[6] Peak voltage is a form of maximum intensity that occurs due to the reflected light from CM in curvature radius where the sensor probe is located. If the position of the sensor probe against the CM surface when producing a peak voltage without solution is called d_p and if there is a solution called d_p', then the presence of a solution such as a convex lens on the surface of the CM will make the d_p' value smaller than d_p. This is shown in Figure 1B which illustrates the light trajectory of the sensor probe-sample-CM-sample probe-sensor probe with the probe sensor position located at the curvature radius of CM. Light comes into the sample (black line), partially reflected by the sample surface (blue line) and partly refracted by the sample to the CM surface. The reflected light from the CM will be refracted by the sample to the sensor probe. The trajectory of light representing in and out of the sample is illustrated by a red line.

The sensor working mechanism is based on the displacement sensor. The shift of the sensor probe to the reference point near the sample surface (D) will produce a peak voltage (V_p). Since the rhodamine B solution absorbs the source light used (wavelength of 543 nm) and the rhodamine B concentration change in the order of tens of ppm does not alter its refractive index value,[6] the detection mechanism uses the absorption principle and change in the concentration of rhodamine B will change the V_p value. On the other hand, the light intensity reflected by the surface of the rhodamine B solution that reentered the sensor probe did not change (Fresnel reflection principle). The volume of the rhodamine B solution was made almost twice the CM volume so that the optical path in the sample is longer. This will result in the higher light absorption and greater sensor sensitivity.

3 | EXPERIMENT

The schematic experimental setup for the sensor of rhodamine B concentration is shown in Figure 2. It consists of a laser He-Ne (with wavelength 543 nm and maximum power of 5 mW) as a light source, fiber coupler used multimode structured 2 × 2 made of plastic (1 mm diameter fiber and 2.2 mm with jacket, 1 m length, 50/50 split ratio, 3.7-5.6 dB insertion loss, and 1.6 dB excess loss), a silicon photo detector as an optical detector with a digital voltmeter to read the detector output voltage. XYZ stage with a displacement resolution of 10 μm and range of 25 mm is used to shift the probe sensor. CM is used in this research as reflector as well as a sample container consisting of two types, namely CMR9 with curvature radius and diameter of 9 mm (volume CM 39 μl) and CMR12 with curvature radius and diameter of 12 mm (volume CM 92 μl). Two micropipettes (size
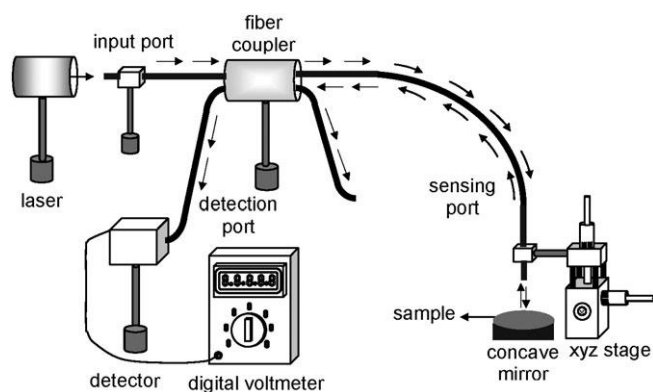
FIGURE 2 Experimental set-up of sensor of rhodamine B concentration using fiber coupler and CM

10-100 µl and 100-1000 µl) were used to measure the volume and place the sample on the container. Rhodamine B solution with distilled water solvent as sample in our experiment had a concentration of 0-20 ppm with variation of 2 ppm.

The first step of experiment is to characterize the absorption spectrum of rhodamine B solution using a UV-Vis spectrophotometer and measuring the refractive index of each sample of rhodamine B using the Abbe Refractometer. After ensuring that the absorption properties of the rhodamine B solution suitable for sensor using absorption principle, the experiment was continued by placing the sample using a micropipette in the sample container CMR9 with an experimental setup such as Figure 2. Volume of sample was set at 70 µl (slightly smaller than twice of CM volume) so that the sample does not spill from the sample container. Next step is to place the sensor probe in the middle of CMR9 which is about 0.5 mm from the sample surface on the main axis of the CM. This position is acting as the reference point of the probe shift. This step is to guarantee that the probe is not in contact with the sample. Recording the detector output voltage was carried out, every sensor probe is shifted 100 µm away from the sample surface. The experimental procedure was performed for each sample concentration selected and control (without sample) with repetition of three times for each sample. Furthermore, the same procedure was
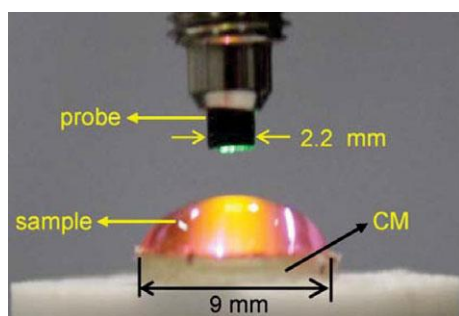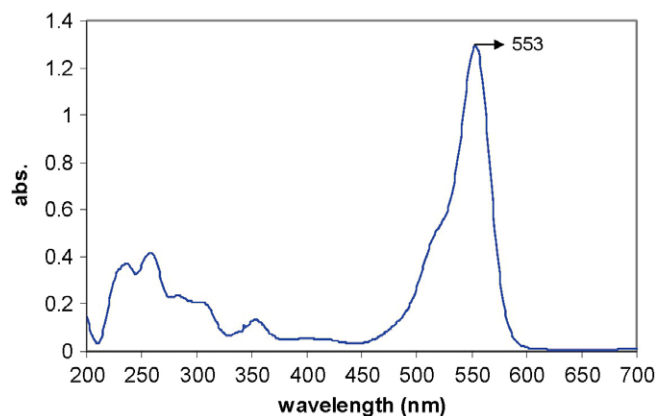

FIGURE 3 Photograph of rhodamine B solution in CMR9 container (photo taken using DSLR camera) [Color figure can be viewed at wileyonlinelibrary.com]

conducted using CMR12 using sample with volume of 170 µl. The last step of experiment was sensor stability test. The sensor stability test was performed by placing the sensor probe in the position where the sensor produces a peak voltage. The recording of peak voltage was conducted every 30 seconds for 15 minutes. The sensor stability test was performed on each sample concentration. All experiment procedures were carried out at a constant room temperature of 24°C.
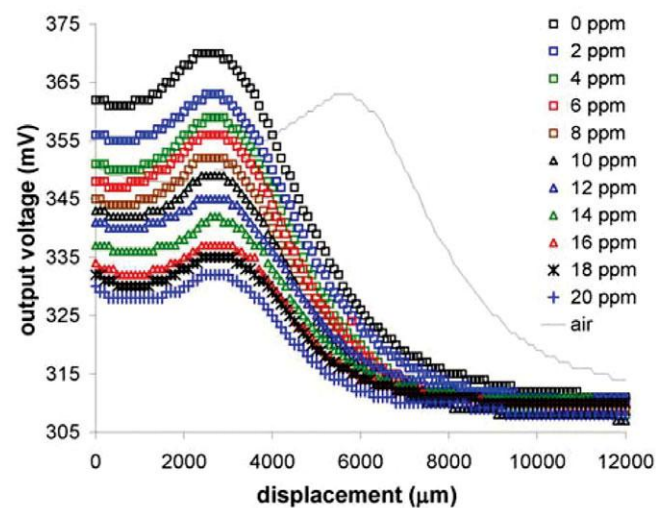
4 | RESULTS AND DISCUSSION

The photograph of sample with volume 70 µl on CMR9 sample container is shown in Figure 3. The shape of the sample is shown clearly like a convex lens. The result of absorption spectrum of rhodamine B with concentration of 10 ppm is shown in Figure 4. The absorption of rhodamine B solution at light source wavelength of 543 nm is 1.03 ABS (90.67%). From measurement, refractive index for each concentration of rhodamine B solution used in our experiments is similar and equal to 1.333. Thus, the sample of rhodamine B solution is in accordance with the working principle of absorption based sensor.
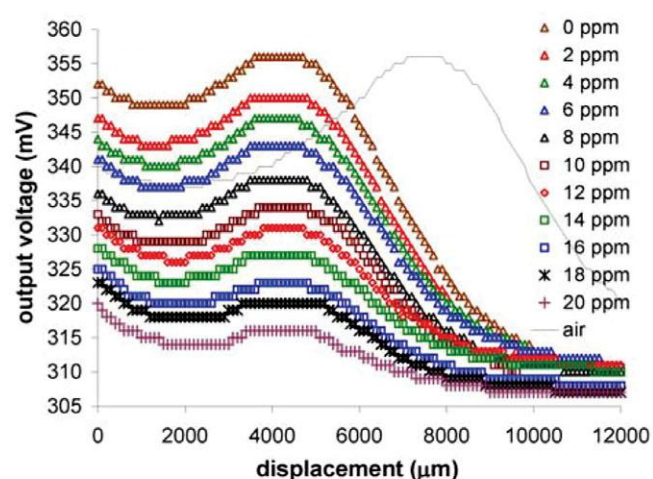
The result of detection of rhodamine B concentration in distilled water was in the form of optical detector output voltage as a function of probe sensor shift to the reference point near the rhodamine B (D) solution for each concentration selected. The data are shown through the curve of the detector output voltage against the sensor probe shift in Figures 4A,B respectively for the use of CMR9 and CMR12. The largest measurement error for set-up using CMR9 and CMR12 is the same of 1.2 mV (0.01%). The reference point (point 0 in Figure 4) is 0.5 mm from the sample surface. The position of the sensor probe against the reference point when producing the peak voltage (D_p) is not at one point, but at a certain distance range. From the data generated, the average D_p for CMR9 and CMR12 usage was found as 2.7 mm and 4.2 mm, respectively. The sample volumes in the experiments using CMR9 and CMR12 are 90% and 92% of the maximum volume that the sample container can accommodate. From the calculation, if the sample volume is assumed to be precisely the maximum volume of the sample container (twice of CM volume), the sample thicknesses on the CMR9 and CMR12 axes are 2.4 mm and 3.2 mm, respectively. For control experiment, the averages D_p generated were 5.6 mm and 7.5 mm for CMR9 and CMR12, respectively. If coupled with the sample thickness on the principal axis of CM and the reference point, the experimental D_p values are 8.5 mm and 11.2 mm for CMR9 and CMR12, respectively. The value is close to the radius of curvature of CMR9 and CMR12. For experiments using samples, if the mean D_p values obtained is the sum of sample thickness on the primary axis of CM and the reference point, then the resulting D_p values for set-up using CMR9 and CMR12 are 5.6 mm

FIGURE 4 The absorption spectra of rhodamine B solution with concentration of 10 ppm [Color figure can be viewed at wileyonlinelibrary.com]

(A)

(B)

FIGURE 6 Graph of the average peak voltage position against the concentration of rhodamine B for set-up using (A) CMR9 and (B) CMR12
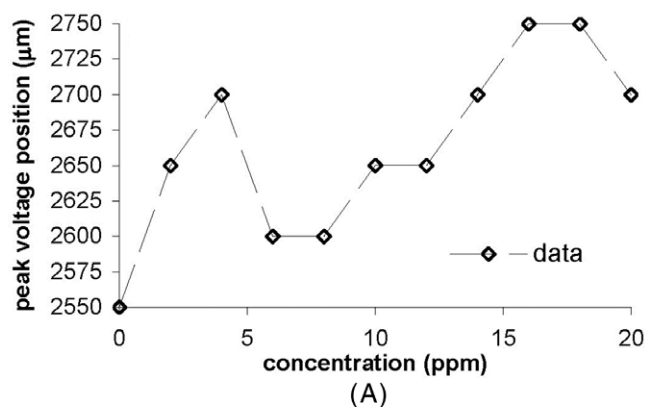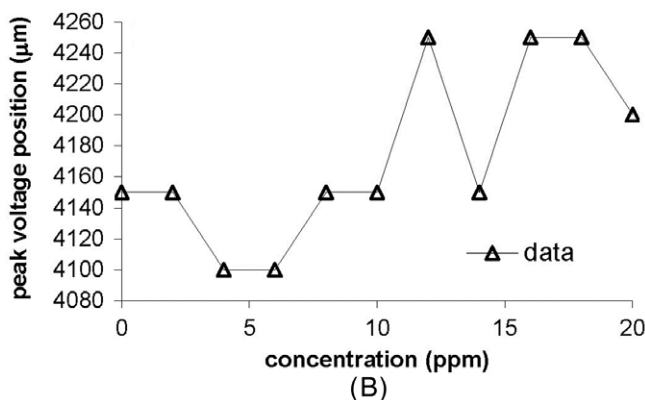

(A)

(B)

FIGURE 5 Graph of the detector output voltage against the surface of the rhodamine B solution with different concentrations using (A) CMR9 and (B) CMR12 [Color figure can be viewed at wileyonlinelibrary.com]

and 7.9 mm, respectively. Decrease in the probe position of the sensor against the CM surface occurs when it produces a peak voltage if the sample justifies of the illustration of the light trajectory in Figure 1B.

Based on the data shown in Figure 5, the change in rhodamine B concentration affects both D_p and V_p values. The connection between average of D_p and V_p against the concentrations of rhodamine B is presented in Figures 6 and 7. In Figure 6, it can be seen that there is inconsistent or random connection between D_p and rhodamine B concentration. From the data, it can be concluded that the concentration of rhodamine B cannot be detected through the average of D_p. Meanwhile, from the data in Figure 7, it can be seen that there is a linear connection between V_p and rhodamine B concentration with a linearity level of more than 99% for both set-up using CMR9 and CMR12. That is, the concentration of rhodamine B can be detected through V_p resulting from the probe sensor shift on the sample surface. Our test to the sensor shows that the working area of the sensor (linear region) is 0-20 ppm. The linear slope in Figure 7 is the sensor sensitivity value.

Sensor stability test results using containers of CMR9 and CMR12 are shown in Figure 8. The test results show that the proposed sensor has good stability. The largest SD resulting from the sensor stability test for CMR9 and CMR12 has the same value, which is 0.5 mV. From the SD
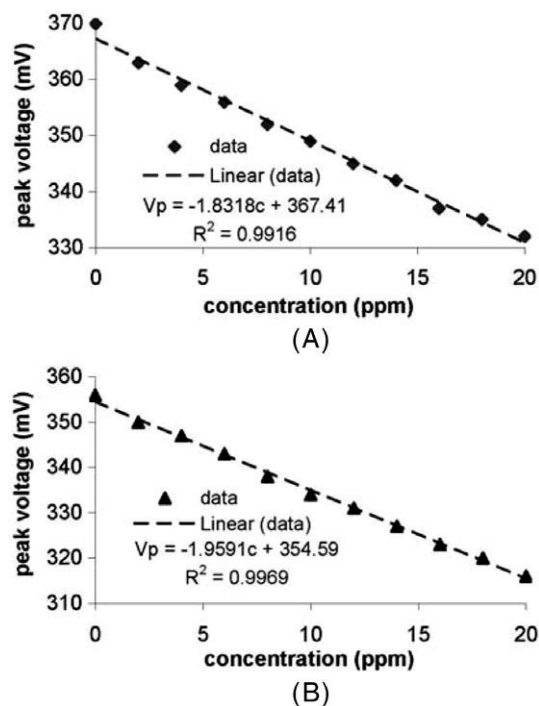
FIGURE 7 Graph of peak voltage values against the concentration of rhodamine B for (A) CMR9 and (B) CMR12

and sensitivity values of the sensors, we can calculate the sensor resolution value of 0.27 ppm and 0.26 ppm for CMR9 and CMR12, respectively. The sensor resolution for set-up using CMR12 is slightly better because the optical path traversed by the light is longer.

Overall, the performance of the rhodamine B concentration sensor in the distilled water is shown in Table 1. From sensitivity and resolution parameters, it is known that the performance of the rhodamine B concentration sensor using CMR12 as sample container is slightly better than using CMR9. This result occurs because CMR12 has larger volumes which result in longer optical path. Longer optical path
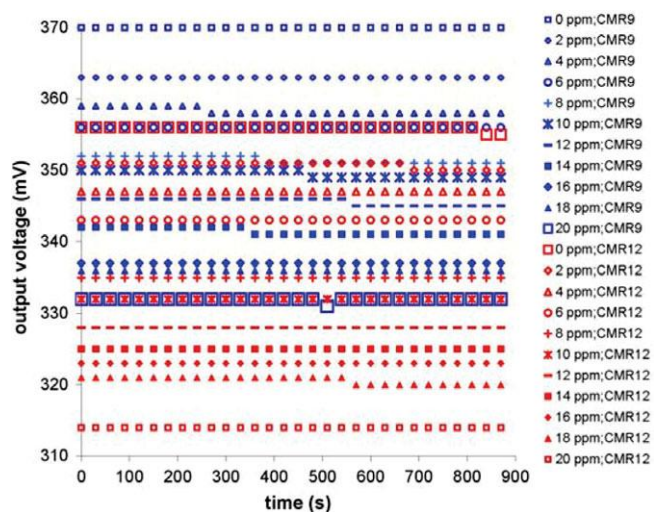
FIGURE 8 Result of sensory stability test for (A) CMR9 and (B) CMR12 [Color figure can be viewed at wileyonlinelibrary.com]

TABLE 1 Characteristics of rhodamine B concentration sensor using fiber coupler, CMR9, and CMR12 as reflectors as well as sample containers

Parameters	Value	
	CMR9	CMR12
Sensor range, ppm	0-20	0-20
Linear region, ppm	0-20	0-20
Sensitivity, mV/ppm	1.83	1.96
Resolution, ppm	0.27	0.26

causes greater light absorption by the sample. As the work mechanism of sensor uses the principle of absorption, then at the same concentration of rhodamine B, rhodamine B absorption using CMR12 is higher than absorption using CMR9.

As it is known, rhodamine B is a textile dye that is widely misused for food or beverage dye in Indonesia.[6] If it is consumed into the human body, it can be harmful to health (zero tolerance). Therefore, rhodamine B concentrations sensor for low concentration is more urgent to be developed than sensor for higher concentration. For this reason, the experiment is carried out with an upper limit of 20 ppm. Referring to Figure 5, in particular the use of CMR9, the largest detection limits can still be increased (seen from the lowest V_p generated.) Although the resolution of sensor generated in this experiment (0.26 ppm) is no better than the previous research result of 0.02 ppm,[6] our proposed sensor has advantage that the detection can be conducted without contact between the sensor probe and sample. This advantage makes the sensor more durable and easier to maintenance. Theoretically, our sensor can be used to detect other substance concentration as long as the detected solution is meniscus and has high light absorption in specific wavelength.

5 | CONCLUSION

Detection of rhodamine B concentration in distilled water using fiber coupler and CM by applying the principle of light absorption can be conducted without contact between the sensor probe and the sample (non-touch). Based on the displacement sensor, the concentration of rhodamine B was detected in the range of 0-20 ppm with a resolution of 0.26 ppm through the peak value of optical detector voltage obtained from the shift of sensor probe against the sample surface.

ORCID

Samian https://orcid.org/0000-0001-5395-2935

REFERENCES

[1] Govindan G, Raj SG, Sastikumar D. Measurement of refractive index of liquids using fiber optic displacement sensors. *J Am Sci.* 2009;5(2):13-17.

[2] Yasin M, Soelistiono S, Yhun Yhuwana YG, et al. Intensity based optical fiber sensors for calcium detection. *J Optoelectron Adv Mater.* 2015;9(9-10):1185-1189.

[3] Rahman HA, Harun SW, Yasin M, Ahmad H. Fiber-optic salinity sensor using fiber-optic displacement measurement with flat and concave mirror. *IEEE J Select Top Quant Electron.* 2012;18(5): 1529-1533.

[4] Binu S, Mahadevan Pillai VP, Pradeepkumar V, Padhy BB, Joseph CS, Chandrasekaran N. Fibre optic glucose sensor. *Mater Sci Eng C.* 2009;29:183-186.

[5] Yasin M, Samian FN. Aini, fiber optic coupler displacement sensor for detection of glucose concentration in distilled water. *J Optoelectron Adv Mater Rapid Commun.* 2016; 10(5-6):347-350.

[6] Samian AH, Zaidan M. Yasin, detection of rhodamine B levels in distilled water based on displacement sensor using fiber coupler and concave mirror. *J Optoelectron Adv Mater.* 2016;18(11-12):988-992.

[7] Yasin M, Samian M. Khasanah. Detection of magnesium ion concentration using fiber coupler based displacement sensor with concave mirror target. *Optik.* 2018;158:37-43.

[8] George NA, Paul AM, Saranya MS. Microbend fiber optic detection of continuously varying refractive index of chlorinated water. *Optik.* 2014;125:301-303.

[9] Hazli Rafis N, Irawati HA, Rafaie H, Ahmad SW, Harun RM. Nor, detection of different concentrations of uric acid using tapered silica optical sensor coated with zinc oxide (ZnO). *J Teknol.* 2015;74(8):55-58.

[10] Kant R, Tabassum R, Gupta BD. Fiber optic SPR based uric acid biosensor using uricase entrapped polyacrylamide gel. *IEEE.* 2016;28(19):2050-2053.

[11] Tabassum R, Gupta BD. Fiber optic manganese ion using SPR nanocomposite of ZnO-polypyrrol. *Sens Actuators.* 2015;B220: 903-909.